

First Experimental Results of a Grid Connected Vertical Axis Marine Current Turbine using a Multilevel Power Converter

Johan Forslund* and Karin Thomas

Division of Electricity, Department of Engineering Sciences, Uppsala University
The Ångström Laboratory, Uppsala, Sweden

*johan.forslund@angstrom.uu.se

Abstract—An experimental marine current power station has been deployed in Söderfors, Sweden. It comprises a vertical axis turbine directly connected to a permanent magnet synchronous generator rated at 7.5 kW. The generator is controlled by a Back-To-Back 2L-3L Cascaded H-Bridge full scale bi-directional Power Converter located on shore. This paper presents the first test results of the power converter, including grid connection. The startup of the turbine, power extraction and initial active power injection to the grid, at 50 % of rated power, operated as predicted by laboratory experiments and simulations. After 40 seconds of grid connection the safety system disconnect the grid converter due to high currents injected to the grid. The problem is mostly likely associated with the current controller in the dq0 frame. Further tuning of the PI regulators and the potential addition of an anti-windup could mitigate the control issue.

Index Terms—Grid Connection, Multi-Level Converter, Hydrokinetic Energy, Vertical Axis Turbine, Low-Speed Generator.

I. INTRODUCTION

Marine current power utilizes the kinetic energy in free-flowing water. One of the main advantages of tidal power, besides being renewable, is its predictability, and one of the main draw backs is the variation of water speed throughout any given day. To be able to utilize as much as possible of the kinetic energy, the power take-off device must be efficient at low power and at the same time rated for handling high power. The power converter must be able to control the power take-off device and convert the power into electricity that follows grid code and standards.

In this paper, a Back-To-Back 2L-3L Cascaded H-Bridge full scale bi-directional Power Converter is investigated. The proposed design is intended to be easily scaled up and to be used for connecting several turbines using one shared DC-link. Most vertical axis turbines are not self-starting, which means that the power converter will need bi-directional in order to both be able to supply the generator with power and to inject power to the grid. The generator side converter is run as an active boost rectifier during grid connection. Using an active rectifier, as opposed to a passive, reduces lower frequency harmonics and allows for boosting and control of the output DC voltage [1]. During startup, the generator converter is run as a two-level inverter. For the grid side, a multi-level

converter has been chosen. It adds complexity to the system but reduces the high-frequency harmonics produced by the switching components [2], [3].

In this paper, test results of a first successful grid connection of a full-scale bi-directional power converter is presented. The Division of Electricity at Uppsala University has developed a test site for hydrokinetic energy conversion in the river Dalälven in Söderfors. A Vertical Axis Turbine is connected directly to a Permanent Magnet Synchronous Generator (PMSG) placed on the riverbed, see Figure 1, deployed in 2013 [4]. All measurements and control of the marine current energy converter unit is placed on-shore in a measurement cabin just next to the river. Rated operation for the turbine is designed to be at 15 r.p.m. and 1.3 m/s to give an electric output of 7.5 kW. The turbine efficiency, characterized by the $C_P(\lambda)$ -curve, has been experimentally obtained in [5], and shows that the maximum power coefficient for the system (generator and turbine) is $C_{P_{max}} = 0.26$ at optimum tip-speed-ratio $\lambda_{opt} = 3.1$. The nominal values of the turbine and generator can be found in [6], [7] and a more detailed description of the generator design can be found in [8].

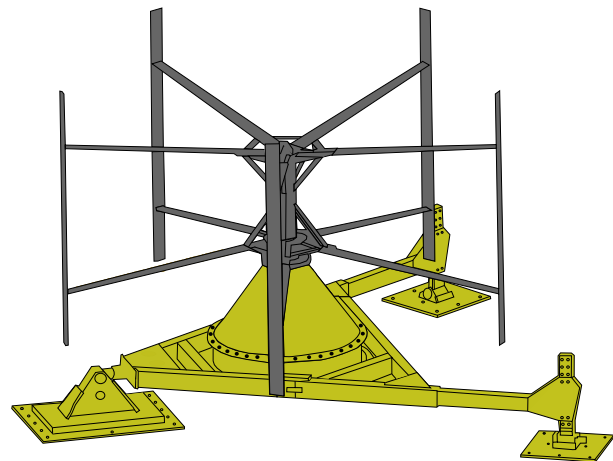


Fig. 1. The Marine current power unit with a vertical axis turbine and generator mounted on the same axis, placed on the riverbed. The Figure is from Figure 5 in [4] (the color scheme has been changed to match the prototype unit). Design by Anders Nilsson.

II. ELECTRICAL SYSTEM AND CONTROL

The following sections will present the basics of the power converter, more details about the design can be found in [9]. The grid connection has been simulated in Simulink and verified in a laboratory setup connected to a generator, presented in [10]. The system consists of a Back-To-Back Two-Level-Three-Level Cascaded H-Bridge converter, with full bi-directional power flow capability, see Figure 2. It uses LCL-filters on both the generator and the grid side before connecting the converters to filter high frequency harmonics and reduce stress on the components. A Y- Δ connected 340/400 V transformer is connected between the grid converter and the grid.

The control system is implemented with LabVIEW and a CompactRIO. The user interface of the program is located on a PC, that through a Real-Time module controls a Field-Programmable Gate Array (FPGA) that handles all time-critical operations at 40 MHz.

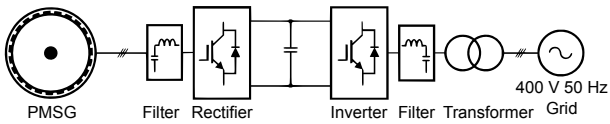


Fig. 2. Overview of the Back-To-Back Power Converter using an active rectifier and a 3L-inverter connected to a shared DC-link. LCL-filters before each converter and a Y- Δ connected 340/400 V transformer is connected between the grid converter and the grid. The Figure is from Figure 3 in [10].

A. Current control of the grid connection

The marine current converter can be operated in three ways; delivering power from the grid to the generator for startup, extracting power from the generator and delivering power to the grid.

During startup the grid converter is operated as a passive rectifier to supply the DC bus with voltage, and the generator converter is run as a BrushLess Direct Current (BLDC) motor with a hysteresis current controller keeping the current in the generator windings between six and ten Amperes per phase. At this point there is no DC bus voltage control.

After the startup, direct-quadrature-zero (dq0) current control is used by applying the Clarke and Park transform of the sensed currents to move the control to the synchronous reference frame (dq0 frame) where PI-regulators are used for d-axis and q-axis current control. The PI regulators are run at 5 kHz, and the constants for the PI regulator are listed in table I.

Both the generator and the grid are assumed to be balanced, so only two of the three-phase currents are used to reduce the computational cost on the FPGA. For the generator converter, the user can set a i_q -axis current reference (active power) and the i_d -axis reference (reactive power) is set to zero. The generator converter operates as an active rectifier that boosts the DC bus voltage. An IGBT with a resistive load, a "chopper", is connected in parallel with the DC bus that engages as soon as the DC bus voltage exceeds 425 V. The

chopper functions as the DC bus voltage limit since the current control has no such control. When the generator converter is activated, but not the grid converter, all extracted power is dissipated in the emergency resistance using the chopper.

When the grid converter is also activated, the i_q -current reference (active power) is set to extract as much power from the DC bus as possible, but still keeping the DC bus voltage at 400 V. The grid i_d -axis current reference (reactive power) is set to zero. The generator i_q -current reference is used as a feed-forward term together with the measured generator frequency to set the i_q -axis reference for the grid side.

TABLE I
PI CONTROLLERS OPERATING AT 5 KHZ

Parameter	Grid currents i_d, i_q	Generator currents i_d, i_q	DC voltage
K_p	-0.0010	-0.0060	-3.99
K_i	-0.0060	-1.2	-3.1
feed forward i_d	0.49	0	
feed forward i_q	-0.68	-0.85	

B. Phase Locked Loop of Grid and Generator Voltages

The current control loops require the position of the measured voltage to move the control into the dq0 frame using Clarke and Park transforms. Synchronous Reference Frame Phase-Locked-Loops (SRF-PLL) run at 10 kHz are used for synchronizing the converter voltages with the measured voltages. The SRF-PLL is sensitive to grid unbalance and harmonics due to the nature of the Clarke and Park transform, [11]. More advanced PLLs can be used, that tracks the positive and negative sequence of the voltage separately, and or includes filter in either the stationary $\alpha\beta$ -frame or the synchronous dq0-frame, see [11]. Here a SRF-PLL is used due to its robustness and low complexity and computational cost. A more in-depth investigation of the SRF-PLL can be found in [12]. Hall sensors are used for calculating the generator frequency and estimating the generator position. In between hall sensors signals the position of the generator is estimated to be linearly dependent on the generator frequency. The PI controller of the SRF-PLL is implemented with an anti-windup scheme. Since the grid voltages are measured after the transformer, but the reference voltages are generated before the transformer, an offset term for the position is necessary and has been experimentally determined in the lab. The same reasoning can be applied to the generator position and its windings, so an offset term for the estimated position is also necessary and was experimentally determined in the lab. See the parameters of both PLLs in Table II.

C. Safety system

The three-phase voltages, currents, and the DC bus Voltage measurements are also used for monitoring for faults. They are checked at 20 kHz and will turn off the corresponding

TABLE II
PLL LOOPS OPERATING AT 10 KHZ

	Grid Voltages	Generator Voltages
K_p	0.0996	
K_i	1	
K_a	1	
θ offset	0.50	0.23

converter. The following limits are set: maximum DC bus voltage at 435 V, maximum generator line current 45 A and maximum grid line current 20 A.

D. Water speed measurements

An acoustic doppler current profiler (ADCP) is placed about 15 m upstream of the turbine to estimate the speed of the water at the turbine. The water speed and distance from the ADCP to the turbine is used to estimate the time delay from the measurement until the measured water speed reaches the turbine. Since the distance is only 15 m, it is assumed there is no change in water speed from the ADCP to the turbine. The ADCP is a Workhorse Sentinel 1200 Hz with an accuracy of 0.3 % of the water speed and is placed at the same depth as the turbine, 7 meters. Measurements are taken every 3 seconds with a bin size of 0.5 meters and give a velocity profile from one meter above the bottom of the river to one meter below the surface.

III. RESULTS AND DISCUSSION

The power converter has been experimentally tested connected to the generator and turbine on-site by; starting the turbine, extracting 50% of rated power from the generator, connecting to the grid and disconnecting first the grid and then the generator. Each test sequence was performed two times with comparable results. The turbine startup, initializing of power extraction from the generator and the initial power injection to the grid behaved as expected in the lab and in simulations in [9], [10]. However, after about 40 seconds of injecting power to the grid, the grid side converter disconnected due to high currents. The results will be discussed in more detail in the following subsections.

A. Water speed measurements

As can be seen in Figure 3, the measured water speeds were in the region of 80 % of the rated speed (1.35 m/s) corresponding to 50 % of rated power (7.5 kW). The variation of water speed is typical for the experimental site. In the Figure, the dashed horizontal blue line represents the rated water speed and the dashed horizontal red line the rated power, assuming a maximum C_P that has been experimentally determined in [5]. The dashed vertical black lines mark the time when the different experiments started. Since the system efficiency is not within the scope of this paper, the water speed and corresponding available power in the water during each region of experiments will not be investigated deeper.

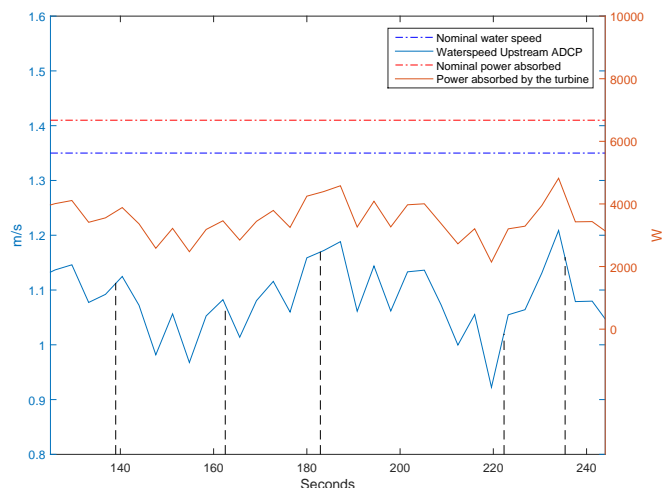


Fig. 3. Water speed during the experiments, the dashed vertical black lines mark the beginning of each experiment. The dashed horizontal blue line represents the rated water speed (1.35 m/s) and the dashed horizontal red line the rated system power (7.5 kW).

B. Startup of the turbine

In the simulations of the startup in [9], the grid side converter was used as an active rectifier to boost the DC link voltage to 400 V. In the current setup, the converter is instead run as a passive rectifier connected to the DC link that supplies the BLDC power to the generator side converter. Figure 4 shows the startup sequence of the turbine. Before the BLDC is engaged, the DC link is charged by the grid to 328 V. The voltage of the DC link decreases as power is injected from the grid via the generator side converter to the generator, forcing the turbine to rotate. Since there is no boosting capability or voltage control of passive rectification, the voltage of the DC link drops as power is delivered to the generator. After a few seconds of BLDC operation, the turbine has reached a rotational speed close to the nominal frequency, which is enough for the turbine to give a net positive torque to the generator and can thus rotate without help from the startup system, at which point the BLDC is turned off. The startup time is comparable with the results found in Figure 7 in the study of the BLDC start of the same vertical axis turbine in [13]. The lack of rotational speed feedback results in an overshoot until a wake has been built up behind the turbine. At high water speeds the overshoot may expose the turbine blades to forces high enough to break connection between the struts and the blades, see [14]. When the BLDC is turned off, the DC link is again charged to 328 V by the grid.

C. Power extraction from the generator

Figure 5 shows the DC bus voltage, power from the generator and the generator frequency when the current reference from the generator is set to an amplitude of 6 A. When the converter starts extracting power from the turbine the frequency of the generator is reduced. The oscillations in generator frequency is a result of the variations of power

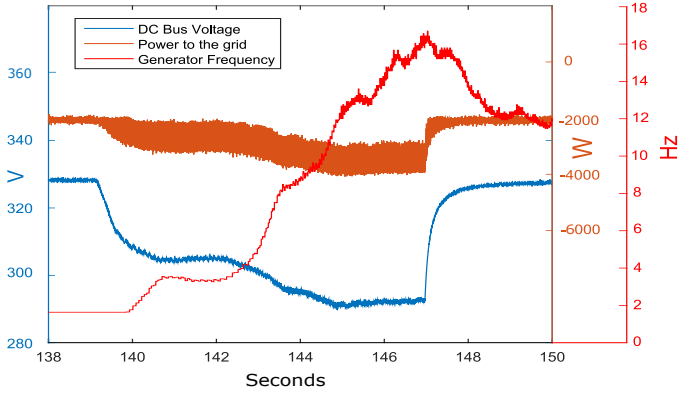


Fig. 4. The startup sequence. The DC link voltage, initially 328 V, is decreased as the grid supplies power to the generator to force the turbine to rotate. Once the turbine has reached a rotational speed close to the nominal frequency the startup is turned off and the DC link is again charged to 328 V by the grid.

absorption by the turbine within each rotation of the turbine. Since the control system sets the current to be extracted from the generator, and does not have any rotational speed feedback, the oscillations cannot be damped by the generator side converter. The DC link is charged to 424 V, with no overshoot. The simulations showed a small overshoot in DC bus voltage when the generator starts extracting power. In this setup, when the generator side converter is activated, the DC bus voltage is lower than what the active rectification will boost the voltage too, removing the possibility of initial overshoot. As can be seen in Figure 6, the spike in amplitude of the initial extracted currents correspond to an overshoot of 74 %, and then reach a stable operating point after a little bit more than one electrical period.

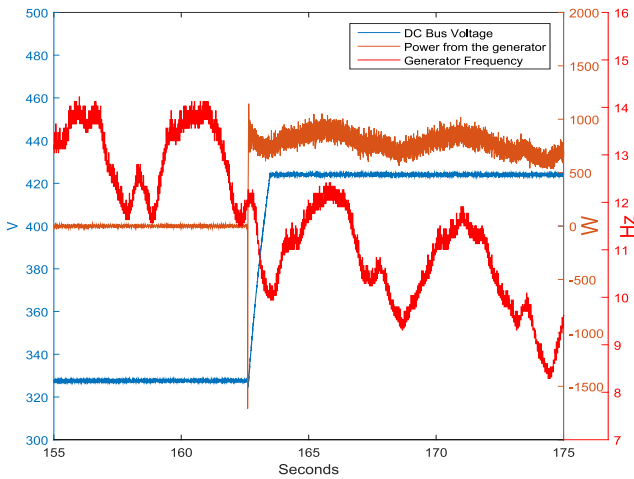


Fig. 5. The generator side converter starts extracting power from the turbine, the DC link is charged to 424 V and the generator frequency decreases (the grid side converter is not yet supplying the grid).

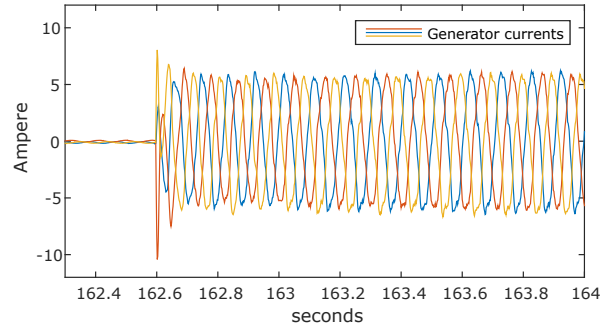


Fig. 6. The currents drawn from the generator as the current reference amplitude is set to 6 A.

D. Power injected to the grid

Figure 7 shows the DC bus voltage, power from the generator and power to the grid when the grid side converter starts injecting power to the grid. The DC link is quickly discharged from 424 V to the set point of 400 V and reaches a stable operating point. This means that there is excess energy that is stored in the DC bus capacitors that will be discharged as the voltage is reduced. The discharge of excess energy results in a time slot of 0.2 seconds the grid converter injects more power to the grid than what is extracted from the generator. After that, the grid converter power output follows the generator converter power output. Figure 8 shows the generator and grid currents when the grid side converter starts injecting power to the grid. The grid currents follow the same pattern with an initial overshoot during the discharge of excess energy, and there is no visible change in the generator currents during the grid connection.

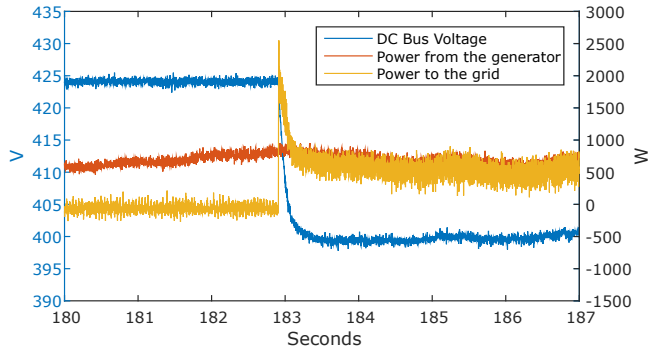


Fig. 7. The grid side converter starts injecting power to the grid. The DC link is discharged from 424 V to 400 V and reaches a stable operating point.

E. Grid side converter disconnected from the grid

After about 40 seconds of grid operation the grid side converter unexpectedly disconnects from the grid. Figure 9 shows the DC bus voltage, power from the generator and power to the grid during the disconnect. The generator converter continues to extract power after and during the fault, as can also be confirmed by looking at the generator currents in Figure 10.

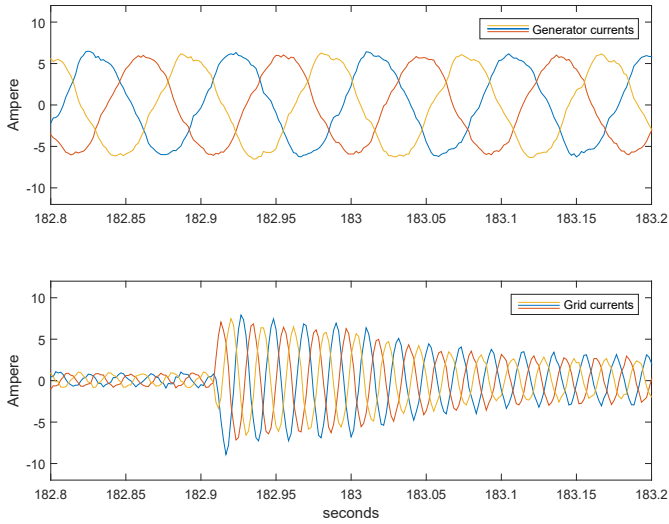


Fig. 8. The grid side converter starts injecting power to the grid.

Before the grid is disconnected there is a drop in the DC link voltage. Once the grid converter is disconnected, the generator converter quickly recharges the DC bus to 424 V. Taking a closer look at the behaviour of both the generator and grid side control variables, i_d and i_q , see Figure 11, before the disconnection the only variable that changes is the grid side i_d . The (negative) increase in i_d corresponds to a increase in reactive power injected to the grid. When the grid converter tries to inject more power to the grid than the generator can supply to the DC bus, the DC bus voltage drops. Finally one of the measured instantaneous three phase currents injected to the grid exceeds 20 A so the safety systems disconnects the grid converter. Synchronization with the grid is not lost during the disconnection, as can be seen by that the measured Line-to-Neutral voltage in phase A is in phase with the generated reference voltage, seen in Figure 12. The problem is most likely associated with the i_d -current controller for the grid converter. Either the PI-parameters need further tuning to be adapted for the turbine and generator, or the cause could be integrator windup as a result of the repeated steps of current reference. Integrator windup can be solved by implementing an anti-windup scheme as shown in [15].

F. Power extraction from the generator set to zero

Figure 13 shows the generator currents, voltages, power and DC bus voltage when the current reference for active power extraction from the generator is set to zero. As the current drops to zero there is a spike in the generator voltages most likely caused by the big change in current through the inductance of the generator windings and filter. Even though the current quickly drops to zero, the spike in voltage results in a small peak of power before dropping to zero with a small overshoot.

IV. CONCLUSIONS

The grid connection system has been experimentally tested on-site with a vertical axis turbine and a permanent generator

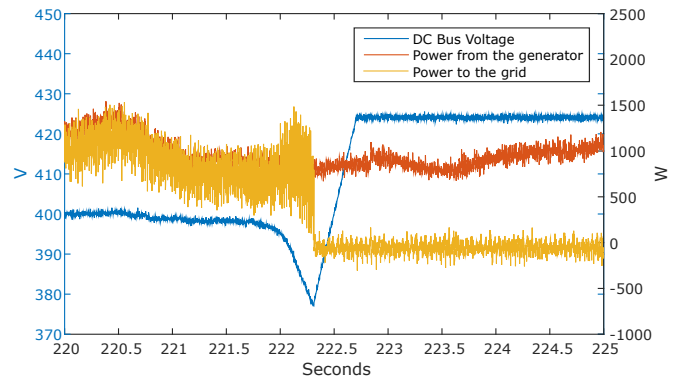


Fig. 9. The safety system unexpectedly stops the grid side converter from injecting power to the grid.

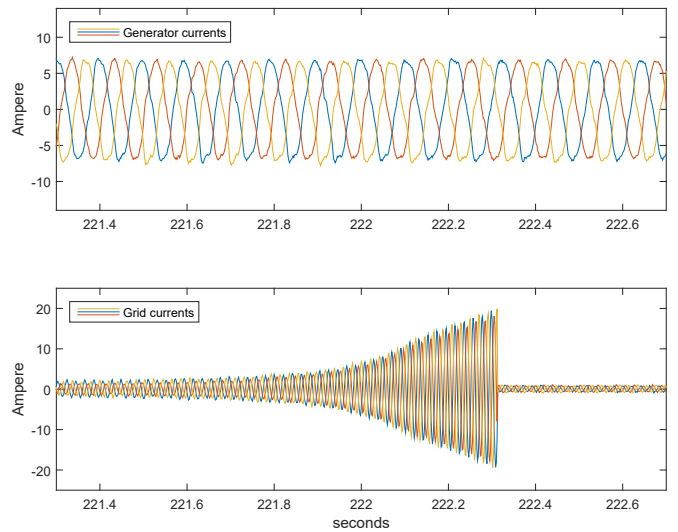


Fig. 10. The generator and grid side currents as the safety system unexpectedly stops the grid side converter from injecting power to the grid.

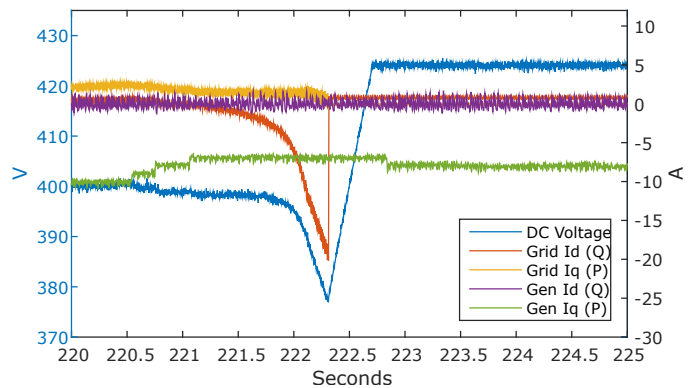


Fig. 11. The DC bus voltage, i_d and i_q controls of the generator and grid currents. The i_d -current increases rapidly until 20 A when the safety system disconnects the grid converter.

placed on the bottom of a river bed. The water speed during the experiments corresponds to about 50 % of the rated power, 7.5 kW, of the turbine and generator. The system operates

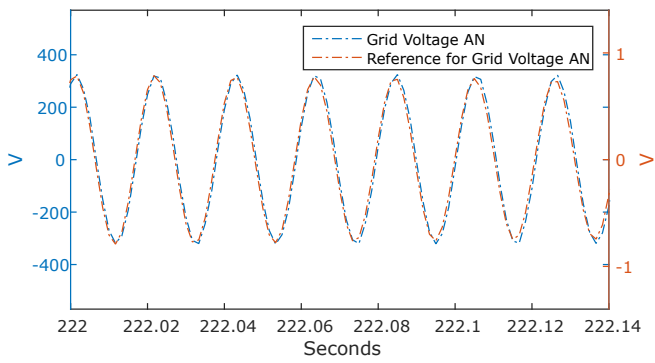


Fig. 12. The measured Line-to-Neutral grid voltage in phase A compared to the corresponding reference voltage created for the converter just before the fault.

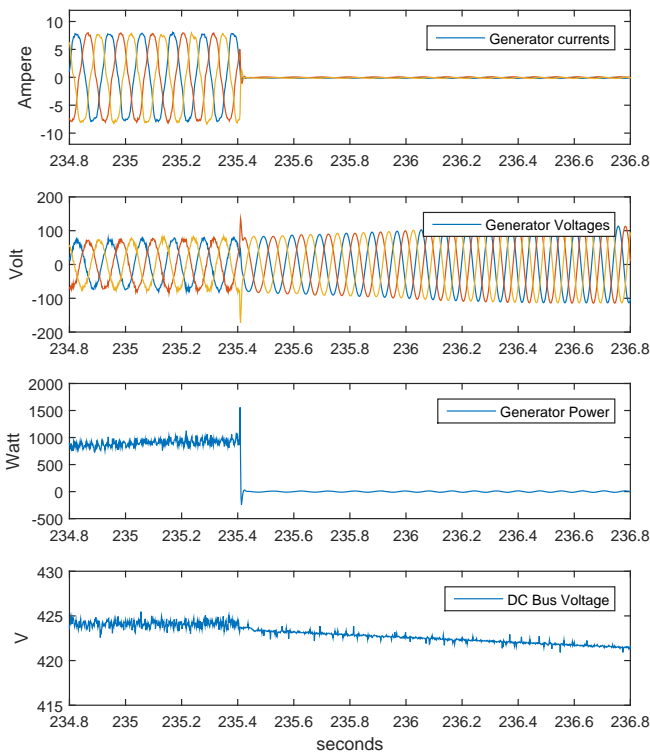


Fig. 13. The generator side current reference is set to zero, no more power is extracted from the generator.

satisfactory during the startup of the turbine, power extraction from the generator and initially during injection of power to the grid. After around 40 seconds of grid connection, a sudden spike in reactive power, supplied by the grid side converter to the grid, forces the safety system to disconnect the grid converter. The generator side converter remains unaffected during the disconnection. The problem is most likely associated with the grid side current controller that either needs more tuning of the PI regulators or an anti-windup. For both the generator and grid side current controllers, the PI regulators are quite aggressively tuned. The response is therefore very fast, but the fast changes in current may lead to voltage spikes due to

the inductances of the filters on each side of the DC bus or to overshooting of currents that can cause unwanted power or voltage fluctuations.

ACKNOWLEDGMENTS

The work was supported by Vattenfall AB, STandUP for Energy, Ångpanneföreningen's Foundation for Research and Development (ÅForsk) and the J. Gust. Richert Foundation. Thank you Senad Apelfröjd and Martin Fregelius for the design and construction of the grid connection.

REFERENCES

- [1] R. Wu, S. Dewan, and G. Slemmon, "Analysis of an ac-to-dc voltage source converter using PWM with phase and amplitude control," *IEEE Transactions on Industry Applications*, vol. 27, no. 2, pp. 355 – 364, 1991.
- [2] K. Corzine and Y. Familiant, "New cascaded multilevel H-bridge drive," *IEEE Transactions on Power Electronics*, vol. 17, no. 1, pp. 125–131, 2002.
- [3] M. Malinowski, K. Gopakumar, J. Rodriguez, and M. Prez, "A survey on cascaded multilevel inverters," *IEEE Transactions on Industrial Electronics*, vol. 57, no. 7, pp. 2197 – 2206, 2010.
- [4] S. Lundin, J. Forslund, N. Carpman, M. Grabbe, K. Yuen, S. Apelfröjd, A. Goude, and M. Leijon, "The Söderfors project: Experimental hydrokinetic power station deployment and first results," in *Proceedings of the 10th European Wave and Tidal Energy Conference, EWTEC13, Aalborg, Denmark, 2–5 September 2013*.
- [5] S. Lundin, J. Forslund, A. Goude, M. Grabbe, K. Yuen, and M. Leijon, "Experimental demonstration of performance of a vertical axis marine current turbine in a river," *Journal of Renewable and Sustainable Energy*, vol. 8, no. 6, pp. 064501–1–5, 2016.
- [6] M. Grabbe, K. Yuen, A. Goude, E. Lalander, and M. Leijon, "Design of an experimental setup for hydro-kinetic energy conversion," *International Journal on Hydropower & Dams*, vol. 15, no. 5, pp. 112–116, 2009.
- [7] K. Yuen, S. Lundin, M. Grabbe, E. Lalander, A. Goude, and M. Leijon, "The Söderfors project: Construction of an experimental hydrokinetic power station," in *Proceedings of the 9th European Wave and Tidal Energy Conference, EWTEC11, Southampton, UK, 5-9 September 2011*, pp. 1–5.
- [8] M. Grabbe, K. Yuen, S. Apelfröjd, and M. Leijon, "Efficiency of a directly driven generator for hydrokinetic energy conversion," *Advances in Mechanical Engineering*, vol. 2013, pp. 1–8, 2013, article ID 978140.
- [9] S. Apelfröjd, R. Ekström, K. Thomas, and M. Leijon, "A back-to-back 2L-3L grid integration of a marine current energy converter," *Energies*, vol. 8, pp. 808–820, January 2015.
- [10] S. Apelfröjd, K. Thomas, and M. Leijon, "Experimental verification of a back-to-back 2L-3L grid connection system for a marine current energy converter," in *2nd International Conference on Offshore Renewable Energy (CORE16), Glasgow, UK, September 2016*, pp. 294–299.
- [11] Z. Ali, N. Christofides, L. Hadjidemetriou, E. Kyriakides, Y. Yang, and F. Blaabjerg, "Three-phase phase-locked loop synchronization algorithms for gridconnected renewable energy systems: A review," *Renewable & Sustainable Energy Reviews*, vol. 90, pp. 434–452, 2018.
- [12] S. Golestan and J. Guerrero, "Conventional synchronous reference frame phase-locked loop is an adaptive complex filter," *IEEE Transactions on Industrial Electronics*, vol. 62, no. 3, pp. 1679 – 1682, 2015.
- [13] J. Forslund, K. Thomas, and M. Leijon, "Power and energy needed for starting a vertical axis marine current turbine," in *Proceedings of the 12th European Wave and Tidal Energy Conference, EWTEC17, Cork, Ireland, 27th August – 1st September 2017*.
- [14] S. Lundin, A. Goude, and M. Leijon, "One-dimensional modelling of marine current turbine runaway behaviour," *Energies*, vol. 9, no. 5, pp. 309–1–16, 2016.
- [15] J. Espina, A. Arias, J. Balcells, and C. Ortega, "Speed anti-windup PI strategies review for Field Oriented Control of Permanent Magnet Synchronous Machines," in *Compatibility and Power Electronics 2009, Badajoz, Spain, May 20 - 22, 2009*.